Chapter 19
Applications of Small-Animal Imaging in Neurology and Psychiatry

Cindy Casteels, Habib Zaidi, and Koen Van Laere

1 Introduction

Next to genetical testing and behavioural observations, neuroimaging studies are increasingly performed on primates and rodents to model a variety of human diseases and traits. Animal models of brain disease are available for all major neurodegenerative diseases, epilepsy, stroke, but also psychiatric diseases such as anorexia nervosa, obesity, depression and anxiety [1].

Most commonly, animal models of brain disease are used to elucidate the mechanisms underlying the human condition and to translationally evaluate pharmacological, behavioural or other treatments for the disease. There are at least two criteria that an experimental model must satisfy: (i) reliability and (ii) predictive validity. Even though also other types of validity such as construct, etiological, convergent, discriminant and face validity are relevant to animal models (for an overview see [2]), predictive validity and reliability are the only necessary and sufficient criteria that will justify the model's use for a particular application. Briefly, (i) reliability refers to the consistency and stability with which the disease variables are observed; (ii) predictive validity incorporates specificity of responses to treatments that are effective in the human disease. Undoubtedly, the more types of validity a model satisfies; the greater its value, utility and relevance to the human disorder or condition.

Developing models that fully mimic human neurological or psychiatric disorders is in many cases troublesome. Preclinical studies often need a choice between models that reproduce cardinal pathological features of the disorders by

C. Casteels (✉) • K. Van Laere
Division of Nuclear Medicine, Leuven University Hospital, Leuven, Belgium
e-mail: Cindy.Casteels@med.kuleuven.be; koen.vanlaere@uz.kuleuven.ac.be

H. Zaidi
Department of Radiology & Medical Informatics, Geneva University Hospital, Geneva, Switzerland
e-mail: habib.zaidi@hcuge.ch

H. Zaidi (ed.), *Molecular Imaging of Small Animals: Instrumentation and Applications*,
DOI 10.1007/978-1-4939-0894-3_19,

mechanisms that may not necessarily occur in humans versus models that are based on known pathophysiological mechanisms but may not reproduce all the features seen in patients.

Neurological and psychiatric models can be subdivided in three groups on the basis of the underlying mechanism: (i) genetically engineered; (ii) pharmacology based; or (iii) produced through advanced biotechnology such as viral vector technology. They may encompass several species, both primates and rodents. The use of mice in functional neuroimaging research is limited by the small size of the brain compared to the resolution limitations of current preclinical imaging systems.

The most commonly applied neuroimaging techniques for studying in vivo disease models are positron emission tomography (PET), single-photon emission computed tomography (SPECT) and magnetic resonance imaging (MRI), each of which has its own advantages and disadvantages (see Chaps. 4, 5, and 7). In this chapter, we will focus on how functional imaging technologies (PET and SPECT) have advanced our understanding of human neurological and psychiatric diseases. In particular, we will focus on the role of these techniques in evaluating models of Parkinson's disease, Huntington's disease, Alzheimer, epilepsy, stroke, addiction, depression, mania and eating disorders.

In general, the development of dedicated small-animal PET/SPECT systems offers the ability to study in vivo molecular changes during (i) normal development, (ii) biological processes and responses, and (iii) disease initiation and progression. As such, they may provide surrogate markers and allow assessment of therapeutic interventions by using serial scans over an extended period in the same animal. Selective radioligands for many neurotransmitter receptors [3] and other cellular proteins [4], which act as enzyme substrates [5] or allow the interference of neuronal function [6], are available.

PET imaging offers certain advantages over SPECT including: the acquisition of relatively fast dynamic data (order of seconds) and the potential to quantify these observations [7]. The spatial resolution when compared to structural imaging techniques such as MRI, is relatively limited, with the highest resolution scanners today giving at best 1–2 mm full width at half maximum (FWHM). The sensitivity of dedicated SPECT is typically an order of magnitude lower than PET. The spatial resolution of state-of-the-art preclinical SPECT scanners can be as low as 0.35 mm, although a trade-off between sensitivity and resolution is always needed [8, 9]. However, the detection of pico- and femtomolar concentrations of radioligand is feasible with both PET and SPECT [10].

When designing or performing in vivo small-animal studies of the brain, the following methodological issues must additionally be considered:

- *Motion prevention*:
  - Immobilizing the animal in the PET/SPECT scanner is the first issue that has to be taken into consideration. Although systems and procedures have been developed to use awake monkeys in PET studies [11] and dedicated instrumentation developed to scan rats in their living environment [12], anaesthesia is still the standard for ensuring immobility during in vivo imaging of small-animals. A fundamental requirement of imaging is not to disturb the

biological system under investigation. However, in many instances, anaesthesia can have several effects on the studied brain parameter. These effects are not predictable since changes are often of different magnitude and direction amongst target receptor, enzyme or transporter systems. The choice of anaesthetics is therefore of great importance to investigate, as it needs to minimally interfere with the tracer dynamics and the research question to obtain biologically valid outcomes (see Chap. 18). For example, the anaesthetic isoflurane was found to alter the expression of the plasma membrane dopamine transporter (DAT) in the brain [13], excluding its use for DAT imaging. Matsumara et al. investigated the effect of six different anaesthetics agents on the uptake of [^{18}F]-FDG in the rat brain [14] and demonstrated significant effects of the different anaesthetics agents on [^{18}F]-FDG metabolism when administered during the uptake period. Only when anaesthesia was started after the initial uptake phase, i.e. 40 min after [^{18}F]-FDG injection, did the small-animal PET images reflect glucose metabolism of the conscious state, as measured with ex vivo autoradiography [14]. However, delaying the induction of anaesthesia with respect to the administration of the PET ligand is not always possible. It limits imaging to a static state, delays imaging protocol and negates the opportunity for dynamic imaging protocols that are required for fully quantitative and compartmental modelling.

- *Absolute quantification*:
  - Fully quantitative and compartmental modelling is a prerequisite for the accurate determination of various biological parameters, such as receptor density (B_{max}) and affinity (K_D) or derived combined parameters such as binding potential. Kinetic modelling generally requires arterial blood sampling to calculate the blood activity concentration over time (input function) [15]. Techniques that have been established to measure blood activity concentrations in humans need to be carefully considered for animal experiments because the vascular access is more problematic, the blood volume smaller and the heart rate much higher than in humans [16]. Arterial blood sampling in rodents is technically demanding; requires extensive animal preparation, complex catheter manipulation and physiological monitoring. Besides, it hampers serial small-animal PET/SPECT studies over weeks or months. Other techniques deriving the input function from a reference tissue devoid of receptors [17], from images of the heart [18] or from the use of an (arterial) probe [19], have also been developed and could reduce the need for blood sampling. They are, however, highly dependent on the radiotracer used and the molecular target. The last two options, for example, are only feasible when the radiotracer does not undergo significant metabolism [20], or when a standard curve describing the metabolism is usable.
- *Tracer principle*:
  - Assessment of the mass effect of injection is an additional issue, especially in the case of receptor imaging [21]. In human imaging studies, only a small chemical amount of radiotracer is injected, in the range of pico- to microgram.

This dose has several advantages, including conforming to true tracer kinetics and giving lower or negligible toxicity. However, in order to obtain sufficient count rates in the brain of small-animals, relatively high doses need to be injected. Indeed, in small-animal imaging, the increase in dose with increasing resolution and the decrease in dose with decreasing body weight cancel one another. Consequently, the concentration of radioligand in the animal will be higher in the ratio of human to rodent body mass, potentially saturating vulnerable systems. In the case of binding sites of low density such as receptors, the increased mass injected can lead to physiological effects and nonlinear kinetics. One must therefore reduce the injected dose of small-animals as low as possible and necessary.

- *Quantitative analysis*:
  - By its very nature, SPECT and particularly PET are quantitative imaging modalities provided appropriate corrections for physical degrading factors are incorporated in the imaging protocol (see Chap. 17). The automated quantitative assessment of metabolic PET data is attractive and will certainly revolutionize the practice of molecular imaging since it can lower variability across facilities and may enhance the consistency of image interpretation independent of reader experience. For example, the development of tracer-specific small-animal PET probabilistic atlases [22] correlated with anatomical (e.g. MRI) templates enabled automated volume-of-interest (VOI) or voxel-based analysis of small-animal PET data with minimal end-user interaction [23]. One such software tool was developed by Kesner et al. [24] to enable the assessment of the biodistribution of PET tracers using small-animal PET data. This is achieved through non-rigid coregistration of a digital mouse anatomical model with the animal PET image followed by automated calculation of tracer concentrations in 22 predefined VOIs representing the whole body and major organs. The development of advanced anatomical models including both stylized and more realistic voxel-based mouse [25–27] and rat [28, 29] models obtained from serial cryo-sections or dedicated high resolution small-animal CT and MRI scanners will certainly help to support ongoing research in this area [30, 31]. For neuroscience applications, a high-resolution rat brain was also recently developed [32].

2 Applications in Neurology

2.1 Parkinson's Disease

Parkinson's disease (PD) is a progressive neurodegenerative disorder, characterized by massive degeneration of dopaminergic neurons in the substantia nigra (SN) pars compacta [33]. This nigral neuronal loss leads to a striatal dopamine deficiency, which is considered to underlie the most overt symptoms of the disease.

PD affects approximately more than 2 % of the general population over the age of 65. The mean onset of the disease is around 60 years, although up to 10 % of those affected are 45 years of age or younger, referred to as young-onset PD. Clinical signs of PD are evident when about 80 % of striatal dopamine and 50 % of nigral neurons are lost [34].

Traditional models of PD fall into two major categories: (i) pharmacological, for example reserpine or amphetamine administration to deplete dopamine, a largely reversible treatment; and (ii) lesioning using neurotoxins which is permanent, for example intraparenchymal injection of 6-hydroxydopamine (6-OHDA) or systemic administration of 1-methyl-4-phenyl-1,2,3,6-tetrahydropyridine (MPTP), as reviewed by Hantraye et al. [35]. Newer approaches in the development of PD models have been attempted as well based on the identification of monogenic familial forms of the disease (at least 11 different linkages with 6 gene mutations have been identified) [36], resulting in transgenic and non-transgenic experimental models [37]. Each of the abovementioned models have its own strengths and weaknesses in representing the human condition, and have all been extensively characterized behaviourally and neurochemically (for an overview see [38]).

Imaging experimental PD models has largely been in the domain of PET imaging with the availability of radioligands to monitor both pre- and postsynaptic striatal dopaminergic function in order to follow the disease process and to examine compensatory mechanisms. The presynaptic nigrostriatal terminal function can be assessed with radioligands suitable for imaging at least three different functions, (i) aromatic amino acid decarboxylase activity (AADC), (ii) vesicular monoamine transporter type 2 (VMAT2) and (iii) the plasma membrane dopamine transporter (DAT). Imaging of postsynaptic dopaminergic function has focused on the dopamine D_2-like receptor system.

Changes in dopamine metabolism have been widely identified in PD patients and MPTP-treated nonhuman primates using either 6-[^{18}F]-fluoro-L-DOPA ([^{18}F]FDOPA) [39–42] or 6-[^{18}F]-fluoro-L-methyl-tyrosine ([^{18}F]FMT) [43, 44], tracers of catabolism and trapping of dopamine, or its analogs. Somewhat surprisingly, [^{18}F]FDOPA showed no significant brain uptake in the rat [45], although it can be used successfully in vivo in mice [46]. Mouse models of PD, either genetically modified or MPTP-treated, have not been extensively studied with in vivo imaging techniques so far, primarily because of the small size of the brain. However, due to the relatively large size of the striatum, a number of studies have shown that it is feasible. Sharma and colleagues have shown that striatal [^{18}F]FDOPA uptake is reduced in the striatum of homozygous weaver mutant mice (a genetic model of PD) compared to both heterozygous and wild-type control animals [46]. Additionally, homozygous weaver mutant mice show an age-related decline in striatal [^{18}F]FDOPA uptake [47].

Most imaging studies performed in rat PD models measure the loss of presynaptic dopamine terminals primarily using tracers for the DAT using cocaine analogs. After unilateral lesions of the nigrostriatal projection through injection in the medial forebrain bundle (MFB), decreased [^{11}C]-CFT and [^{11}C]RTI-121 binding have been noticed [48], as a result of decreased density of the transporter, without concomitant

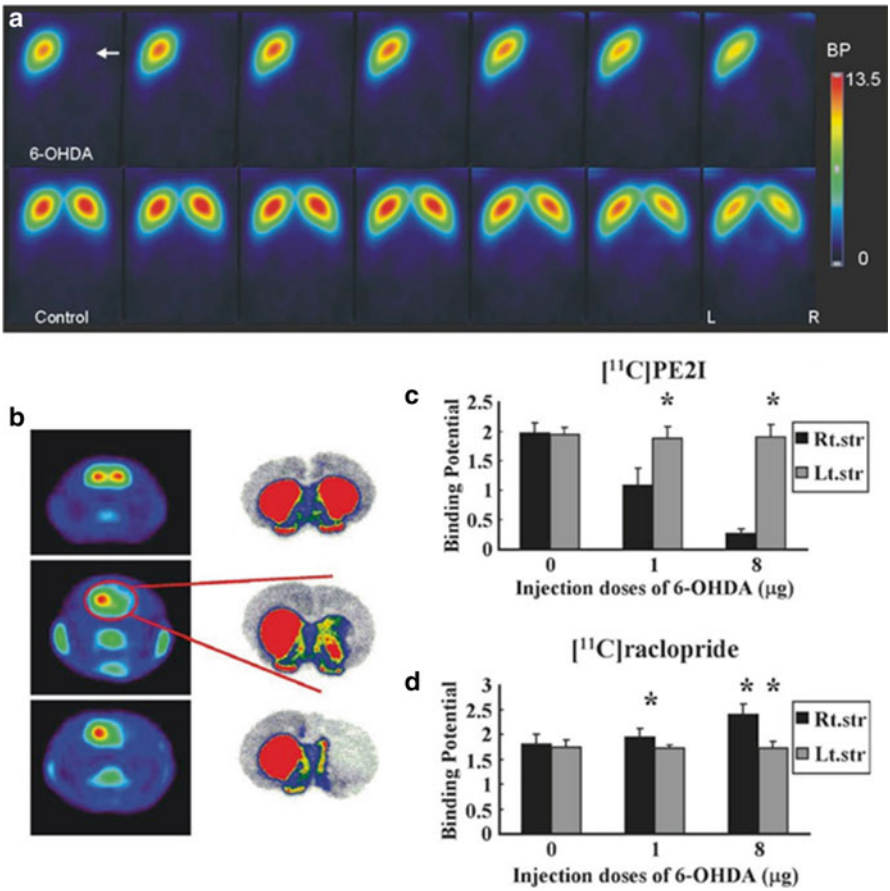

Fig. 19.1 Overview of both pre- and postsynaptic striatal function in the 6-OHDA model of Parkinson's disease. (**a**) Series of axial sections (ventral to dorsal, slice interval 1.0 mm) showing decreased DAT availability in the dorsal striatum of 6-OHDA-treated rats in comparison to controls, as measured using [^{18}F]-FECT. *Color bars* indicate binding indices for the dopamine transporter. (**b**) Also in the same model, reductions in VMAT2 density using [^{11}C]DTBZ with microPET (*left*) and autoradiography (*right*) have been identified. *Top image*: A normal control animal for comparison; *middle image*: an animal with a mild right unilateral lesion; *bottom image*: an animal with a severe right unilateral lesion. (**b**–**d**) PET measures of the integrity of the striatal dopamine function correlates to the amount of 6-OHDA injected. [^{11}C]PE2I binding to DAT (**c**) and [^{11}C]-raclopride binding to D_2 receptors (**d**) decreased and increased, respectively, with injected dose of 6-OHDA. Reprinted from [48, 54, 56] with permission from Springer and Elsevier

changes in affinity [49]. $VMAT_2$ density changes have also been identified (Fig. 19.1b) [48], as have increased [^{11}C]-raclopride binding to the D_2 receptors [50, 51], consistent with human PET studies in early PD patients [52]. Whether the D_2 receptor upregulation is a result of changes in receptor density or affinity is still unresolved, as both characteristics have been found to be altered [51, 53]. Besides, longitudinal microPET analysis of striatal D_2 binding in the same animals

demonstrated that the increase in D_2 receptor density after unilateral 6-OHDA lesions occurs bilaterally [53]. Nikolaus and co-workers found that the D_2 receptor density starts to increase in both striata within 2 days post-lesion, while a trend toward a significant increase in the contralateral striatum was noticed at day 14. The authors attributed the change in the contralateral striatum to be indicative of compensatory changes upon unilateral dopamine depletion [53]. Decreased presynaptic dopamine terminal binding have also been observed after unilateral lesions of the nigrostriatal tract through injection of 6-OHDA in the SN with [^{18}F]-FECT (Fig. 19.1a) [54], and through lentiviral vector-based mediated overexpression of alpha-synuclein in the striatum using [^{123}I]FPCIT [55].

These PET measures of the integrity of the striatal dopamine system have been shown to correlate to the amount of 6-OHDA injected. One study showed that 6-OHDA lesioning causes reciprocal, dose-dependent changes in [^{11}C]PE2I binding to DAT compared to [^{11}C]-raclopride binding to D_2 receptors, decreasing and increasing the binding respectively (Fig. 19.1c, d) [56]. Another study also intended to measure the relationship between the 6-OHDA dose and the integrity of the striatal dopamine system using [^{11}C]DTBZ, confirmed previous correlation [48].

As functional imaging of the striatal dopaminergic system can objectively follow loss of dopamine terminal function in PD, it also provides a potential means of monitoring the efficacy of putative therapeutic strategies. Possible restorative approaches evaluated in PD models include: striatal implants of human and porcine fetal mesencephalic cells, retinal cells that release levodopa/dopamine, embryonic stem cells and neurotrophic factors.

In unilateral 6-OHDA-lesioned rats, striatal transplantation of foetal dopamine neurons restores both the regional cerebral blood volume (rCBV) response to amphetamine as measured with pharmacological MRI, as well as the [^{11}C]CFT binding in the lesioned striatum [57]. Behavioural recovery does not occur until [^{11}C]CFT binding is restored in the same model to 75–85 % of the intact side [58]. The logistic, practical and ethical issues associated with foetal cells, however, contributed to a shift away from this particular line of investigation to the evaluation of alternative source of cells.

Alternative cells such as retinal pigmented epithelial (RPE) cells have so far only been studied in larger animals. RPE cells produce levodopa (L-DOPA), the biochemical precursor of dopamine, as an intermediate in neuromelanin production. Implanted human RPE cells, unilaterally into the striata of bilateral MPTP-treated monkeys, results in improved motor function and increased [^{18}F]-FDOPA uptake with a concomitant decrease in [^{11}C]-raclopride binding 2 months after implant [59].

The potential of embryonic stem (ES) cells as other viable source of cells for transplantation in PD has been evaluated in the unilateral 6-OHDA rat model. Bjorklund et al. [60] have shown that when transplanted into the rat striatum, mouse ES cells differentiate into dopamine neurons and decrease behavioural asymmetries. In addition, [^{11}C]CFT binding was increased in the grafted striatum and correlated with the number of TH+ neurons in the graft [60]. Also in the same model, infusion of GDNF, a neurotrophic factor, into the SN and lateral ventricles prevents the 6-OHDA-induced reduction in DAT, as measured by [^{11}C]-RTI-121 [61, 62].

Despite both histological and PET evidence in animals, neither of the abovementioned graft techniques demonstrated clinical efficacy in controlled trials so far [63, 64]. In those trials "off" period dyskinesias were often problematic. There are suggestions, however, that less severely affected PD patients could benefit more from those intrastriatal implantations.

Apart from the dopaminergic system, another active field of research in recent years has become the study of the contribution of inflammation to the progression of neurodegenerative disorders, as it may provide alternative therapeutic opportunities. Microglia cells are the macrophages of the brain and respond to noxious stimuli by changing morphology and expression of cell-surface markers and releasing pro-inflammatory cytokines [65]. Activated microglia cells may play a major role in the extension of neuronal loss after a lesion or insult. Migration of activated microglia and macrophages towards the lesion site correlates with the secondary damage after an acute neurotoxic event [66]. Moreover, a similar mechanism might amplify and perpetuate neuronal damage in chronic neurodegenerative disorders, such as PD.

Cicchetti and coworkers have used a ^{11}C-labeled tracer that binds to the peripheral benzodiazepine receptor ([^{11}C]-PK11195) to study activated microglia in PD models. Unilateral striatal infusion of 6-OHDA has been shown to increase [^{11}C]-PK11195 binding in the lesioned striatum, at 3 weeks post lesion compared to baseline [67]. In the same model, chronic treatment with a selective inhibitor of the inducible form of cyclooxygenase (COX-2) constrained this inflammatory response at 12 days postlesion and limited, to a certain extent, the progressive dopamine neuronal death in the SN, as measured using [^{11}C]-CFT and immunohistochemistry [68].

Cerebral metabolic mapping with autoradiography has also been used in previous animal research to determine the regional alterations in brain activity related to the pathogenesis of PD [69, 70]. The technique has additionally been used to map regions responsive to levodopa in the 6-OHDA lesioned rat [71]. Nowadays, [^{14}C]-2-deoxyglucose autoradiography is often replaced by [^{18}F]-FDG PET imaging. [^{18}F]-FDG is considered to be a marker of cerebral glucose consumption based on neuronal entrapment and accumulation of [^{18}F]-FDG-6-PO_4, indicating neuronal viability [6]. In PD patients, specific cortical-subcortical metabolic alterations have been described using [^{18}F]-FDG based on direct regional analysis [72] or network analysis approaches [73]. So far, only one study in small-animals has been performed. It was recently demonstrated that the unilateral intranigral lesion produced with 6-OHDA causes a severe metabolic impairment in the ipsilateral sensorymotor cortex of 6-OHDA lesioned rats, while metabolism was relatively increased in the contralateral midbrain, comprising the SN [54]. The change in the contralateral midbrain was attributed to be indicative of compensatory changes to unilateral dopamine depletion, in line with the previous mentioned contralateral D_2 receptor upregulation [53]. It was concluded that the model shows metabolically strong functional correspondence to the cortico-subcortical impairments seen in PD patients [54].

2.2 Huntington's Disease

Huntington's disease (HD), or Huntington's chorea, is an autosomal dominant progressive neurodegenerative disorder affecting approximately 1 in 10,000 individuals and is characterized by involuntary movements such as chorea, emotional disturbances and cognitive impairment [74]. Typically, onset of symptoms occur in middle-age. HD is caused by a cytosine-adenine-guanine (CAG) repeat expansion within exon 1 of the HD gene (IT15) on chromosome 4 [75]. The number of CAG repeats accounts for about 60 % of the variation in age of onset, with the remainder represented by modifying genes and environment [76].

The earliest animal models of HD are based on the selective vulnerability of striatal neurons to excitotoxic amino acids [77]. Intrastriatal injection of quinolinic acid (QA) [78] or systemic administration of 3-nitropropionic acid (3-NP) [79] results in 'pathogenic models' of the disease. Since the recent discovery of the gene mutation for the disease, new transgenic models are also being developed. Transgenic animal models of HD were first created in mice [80] and subsequently in *Drosophila* [81]; later on, a transgenic rat model of HD was reported [82].

Small-animal imaging data on HD are largely PET-based using similar markers described for Parkinson's disease with more experimental data utilizing fluorodeoxyglucose to map regions of reduced metabolism, indicative of cell loss [6]. Imaging of HD models has been used extensively to evaluate both the validity of the models and the effects of various interventions.

In the QA-lesioned rat striatum, [^{18}F]-FDG uptake is substantially decreased at 1 week post lesioning, and decreases further at 5 and 7 weeks postlesion [83]. In contrast, lesion-induced effects on dopamine D_2 receptor binding were more progressive, with an initial upregulation of [^{18}F]-FESP binding apparent 1 week postlesion followed by a decline 5 and 7 weeks thereafter [83]. Additional experiments revealed that the marked upregulation of dopamine D_2 receptors consequent to QA injections could be detected as early as 3 days after the initial insult [83]. Using [^{11}C]KFI8446, Ishiwata et al. have shown that adenosine A_{2A} receptor binding is decreased to a similar extent as [^{11}C]-raclopride binding to D_2 receptors in the lesioned striatum, but to a greater extent than [^{11}C]SCH23390 binding to D_1 receptors [84]. Also in the same model, the QA injury did not affect [^{11}C]flumazenil binding to benzodiazepine receptors at day 5 postlesion [85]. In addition, Moresco et al. have shown that the loss of adenosine A_{2A} and dopamine D_2 receptors are paralleled by an increase of microglia activation, as measured using [^{11}C]PK11195 [86]. At the very first time point investigated, from QA administration (24 h), only a slight non-significant increase in [^{11}C]PK11195 binding was observed. At 8, 30 and 60 days, however, [^{11}C]PK11195 binding values were on average three times higher than the controls.

Compared to intrastriatal QA, repeated systemic administration of 3-NP results in more widespread striatal lesions. A longitudinal [^{18}F]-FDG study aimed to explore the acute and chronic effects of systemic 3-NP administration, showed a significant interanimal variation in response to the toxin [87]. Rats that developed

large striatal lesions had decreased glucose utilization in the striatum and cortex 1 day after starting 3-NP injections. Rats that did not develop lesions showed reversible enhancement in cortical glucose utilization and no changes in striatal glucose metabolism. Progressive degeneration was observed by a decrease in glucose metabolism in the striatum [87].

Transgenic rodents expressing a mutant form of the huntingtin gene are used in the study of disease progression and the effects of treatments. A recent longitudinal study, following up R6/2 mice with [^{18}F]-FDG, demonstrated an exponential decrease in glucose metabolism, starting at the age of 8 weeks and continuing through the 6 weeks follow-up time in the striatum, cortex and cerebellum [88]. Treatment with the transglutaminase inhibitor cystamine in these animals has been shown to have a neuroprotective effect in a dose-dependent manner, attenuating the decrease in striatal, cortical and cerebellar [^{18}F]-FDG [88].

2.3 Alzheimer's Disease

Alzheimer's disease (AD) is the most common cause of progressive cognitive decline in aged humans, comprising 50–70 % of all cases [89]. AD begins with great difficulty in new learning and memory, which leads to forgetfulness of recent events. AD worsens over time, usually over many years, leading to problems in word finding and reasoning, difficulty completing daily activities of living and ultimately death. The most severe neuropathological changes occur in the hippocampus, followed by the association cortices and some subcortical structures, such as the amygdala [90]. The neuropathological changes are characterized by massive neuronal cell and synapse loss [91], as well as beta-amyloid plaques and neurofibrillary lesions [90]. The major protein component of plaques is the polypeptide *Abeta* that is derived from amyloid precursor protein (APP). The neurofibrillary lesions contain hyperphosphorylated aggregates of the microtubule-associated protein *tau* and are found in cell bodies and apical dendrites as neurofibrillary tangles (NFT).

Less than 1 % of the total number of AD cases are caused by autosomal dominant mutations in three genes, among which APP [92]. Mutations in the gene encoding *tau* have also been linked to neurodegeneration and dementia [93]. The fact that these genes encode for proteins that are deposited in plagues and NFTs further confirms their causal role in the disease and led to the generation of transgenic animal models [94]. Most widely used animal models comprise both mouse and invertebrate; rat models of AD are rare. As far as neuro-anatomy, memory and motor functions are concerned, the transgenic mouse models are superior to the invertebrate ones in resembling the human condition [95]. Many different strains exist, but most of these overexpress human APP.

Not all PET studies of transgenic mice have been very successful so far because of the small size of the mouse brain and the inherent limitations in resolution of the first generation of small-animal PET scanners [96]. Considering that [^{18}F]-FDG is becoming one of the most widely used diagnostic adjuncts for AD [97], the

expectation that this technique would also be widely used in transgenic mice has for this reason not been met. Whereas autoradiographic studies show decreased cerebral glucose metabolism in the posterior cingulate cortex, in vivo imaging does not allow the identification of this change [98].

Visualizing Abeta deposition in vivo is another novel diagnostic tool, which might contribute to a definite diagnosis of AD and to monitor the success of treatments. The earliest probe was a dye called BSB (*trans*,*trans*)-1-bromo-2,5-bis-(3-hydroxycarbonyl-4-hydroxy)styrylbenzene, which was used to label Abeta-plaques in Tg2576 mice [99]. In recent years, the novel PET tracer ^{11}C-labeled Pittsburgh Compound-B (PIB) has gained significant attention [100]. PIB was shown to enter the brain quickly and label plaques within minutes [101]. It was used as a PET tracer in APP transgenic mice but initially failed to reflect the amount of Abeta [102]. In APP23 mice, an age-dependent increase in radioligand binding was found to be consistent with progressive Abeta accumulation [103]. Importantly, Abeta reductions upon vaccination with an anti-Abeta-antibody were reflected by reduced binding of [^{11}C]-PIB. The use of transgenic mice in preclinical studies is however limited as species-differences in Abeta accumulation have been reported [103].

In order to diminish the spatial resolution limitations of PET, high-field strength MRI can be combined with preclinical PET imaging for more accurate anatomical localization. In a study combining a transgenic mouse model of AD and the use of the toxin *N*-(2-chloroethyl)-*N*-ethyl-bromo-benzylamine (dsp4), which specifically targets the noradrenergic neurons of the locus coeruleus, Heneka et al. demonstrated an interaction effect between beta-amyloid deposition and noradrenergic neurotransmission [104]. Only transgenic mice who were also treated with dsp4 showed decreased cortex/cerebellum ratios in [^{18}F]-FDG uptake, [^{11}C]flumazenil binding and [^{11}C]*N*-methyl-4-piperidyl-acetate trapping, indicative of reduced cerebral glucose metabolism, decreased neuronal integrity and attenuated acetylcholinesterase activity, respectively.

2.4 Epilepsy

Epilepsy is a common chronic neurological disorder that is characterized by recurrent, unprovoked seizures [105] and affects approximately 3 % of the population during their life-time [106]. Seizures arise from excessive abnormal hypersynchronized firing of a population of cortical neurons [107]. About 60–70 % of patients experience focal or partial seizures, and about 30–40 % generalized seizures [108]. Epileptic seizures are controlled with medication in approximately 70 % of the cases. When seizures are medically intractable, resection of the epileptogenic cortex may be considered.

Many epilepsy syndromes, particularly temporal lobe epilepsy (TLE), are associated with structural and functional abnormalities of the brain. The relationship of these abnormalities to the development (i.e. epileptogenesis), progression and prognosis of epilepsy are still incompletely understood.

Animal models in epilepsy neuroimaging research have long been important for the investigation of the neurobiology, consequences and treatment of seizures and epilepsy. The use of animal models particularly enables the investigation of the neurobiological changes during epileptogenesis, which is difficult to study in humans, given that in most patients, the chronic rather than the early epileptogenic stage is represented. Besides, prospective studies, in which patients at risk are followed up until the onset of the first seizure, are time-consuming, costly and practically difficult to undertake.

The animal models used in epilepsy research can be divided into models of seizures and models of epilepsy itself [109]. In the case of the former, the seizures are induced by the application of an acute brain insult, usually electrical and chemical, while in the latter the seizures occur spontaneously as in human epilepsy. In these chronic models, epileptogenesis is generally induced by a precipitating insult (genetic or acquired) that initiates a cascade of processes that transform a normal to a hyperexcitable epileptic brain, resulting in the occurrence of recurrent spontaneous seizures after a latent or silent period.

In 2000, Kornblum et al. were the first to publish in vivo [^{18}F]-FDG findings during acute seizures using small-animal PET [110]. [^{18}F]-FDG is one of the most commonly used radiotracers for PET imaging in clinical epilepsy practice and research, and is used in patients with refractory epilepsy to presurgically localize the functional deficit zone [111]. In the model of kainic-acid induced seizures, during status epilepticus (SE) a dramatic enhancement in glucose metabolism in several brain regions was demonstrated, most notably in hippocampus and entorhinal cortex [110]. Rats displaying moderate to severe seizures demonstrated 1.6- and 2.3-fold increases in [^{18}F]-FDG uptake in the hippocampus, respectively. This correlation between [^{18}F]-FDG uptake and seizure activity was also confirmed in C57BI/6 mice [112]. Using pilocarpine induced SE in these animals, [^{18}F]-FDG uptake in the hippocampus (+33.2 %) was directly correlated with seizure activity during the uptake period.

Wang et al. studied a mouse model for GLUT-1 haploinsufficiency using [^{18}F]-FDG small-animal PET [113]. GLUT-1 is the predominant glucose transporter expressed in the blood–brain barrier and is responsible for glucose entry into the brain [114]. GLUT-1 haploinsufficient mice were found to display among others spontaneous epileptiform discharges on electroencephalography, paralleled by a diffuse hypometabolism in the brain as compared to the wild-type strain [113].

Recently, longitudinal small-animal PET imaging was used to study brain glucose metabolism during epileptogenesis in two chronic epilepsy models of TLE [115]. In the amygdala kindling model, rats were found to have decreased glucose uptake in the ipsilateral hippocampus at the end of the kindling period that persisted at the 2 weeks post-kindling scan. In the post kainic acid induced SE model, a global hypometabolism was presented as early as 24 h after the kainic acid treatment. This hypometabolism remained persistently decreased for the following 6 weeks and was not affected by the onset of spontaneous seizures.

More recently, the relationship between brain glucose metabolism and epileptogenesis was further investigated in the rat lithium-pilocarpine model of epilepsy

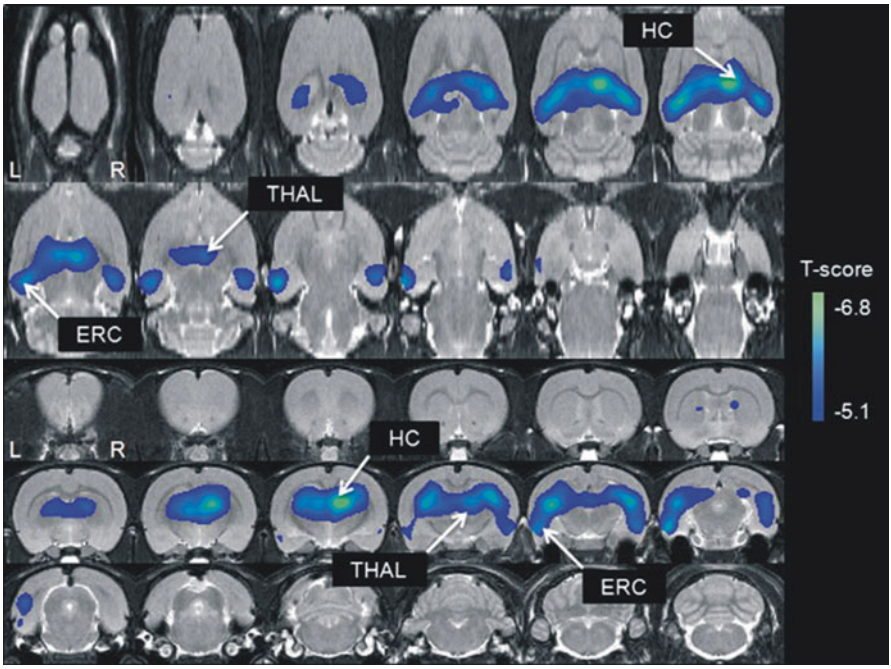

Fig. 19.2 Comparison of brain glucose metabolism between SE and control animals on day 3. Differences for the brain regions have been color-coded and are superimposed on a MRI template. Axial (*top 2 rows*) and coronal (*bottom 3 rows*) brain sections showing significantly decreased [^{18}F]-FDG uptake on day 3 in SE rats compared to controls, most pronounced in hippocampus (*HC*), entorhinal cortex (*ERC*) and thalamus (*THAL*) bilaterally (*white arrows*). Significance at the voxel level is shown with a T statistic color scale. Reprinted from [116], with permission from Elsevier

using a voxel-based analysis approach [116]. Early in the silent phase of epileptogenesis (day 3), rats displayed a severely hypometabolism in the entire cerebrum, although no electro-encephalographic or behavioural seizure activity was present at that time. This hypometabolism was most pronounced in the hippocampus, entorhinal cortex and thalamus bilaterally (Fig. 19.2); regions all characterized by the highest [^{18}F]-FDG uptake during SE. During the chronic epileptic phase, a normalization of the glucose metabolism was seen.

Apart from [^{18}F]-FDG, as marker of neuronal activity, specific neurochemical changes can be measured by the use of specific receptor ligands. Several of these receptor systems represent existing or possible therapeutic targets.

The receptor that has most commonly been imaged using PET in human epilepsy studies has been the central benzodiazepine (cBZ) receptor using radiolabeled flumazenil (FMZ). Changes in expression and function of the $GABA_A$/cBZ receptor complex are well described in human focal epilepsy [111]. Liefaard et al. used a population pharmacokinetic model to study the changes in GABAa/cBZ complex in the kindling model of TLE [117]. After injection of an excess amount of [^{11}C]FMZ

to fully saturate the receptors, the concentration-time curves of [^{11}C]FMZ in blood and brain were measured, from which K_D and B_{max} were estimated. After kindling, K_D was unaffected, but B_{max} in epileptic rats decreased to 64 % of controls. Also in fully kindled rats, the brain volume of distribution was found to be increased with 180 %, indicating, in these animals, reductions in transport of [^{11}C]FMZ outside the brain [117].

Another receptor radiotracer with potential for small-animal epilepsy models is (*N*-[2-(3-cyano-phenyl)-3-(4-(2-[^{18}F]fluorethoxy)phenyl)-1-methylpropyl]-2-(5-methyl-2-pyridyloxy)-2-methyl proponamide) ([^{18}F]MK-9470), which labels brain type 1 cannabinoid (CB_1) receptors [3]. Cerebral CB_1 receptors belong to the endocannabinoid system (ECS), together with a family of naturally occurring lipids, the endocannabinoids, and with transport and degradation proteins [118]. The endocannabinoid system would provide an 'on-demand' protection against acute excitotoxicity in neurons of the central nervous system and would contribute to a signaling system that protects neurons against the consequences of abnormal discharge activity [119]. In rodent models of epilepsy, administration of cannabinoids is protective against seizures [120, 121] and affects seizures' frequency and duration. Endocannabinoids and CB_1 receptor levels are increased in these epileptic animals [122]. Using small-animal PET, the involvement of the ECS was recently demonstrated, more precisely the CB_1 receptor, in the mechanism-of-action of the antiepileptic drug valproate (VPA) [123]. A significant increase (+32 %) was found in global cerebral [^{18}F]MK-9470 binding after 2-week chronic VPA administration compared to sham-treated animals. As VPA does not exhibit high affinity for the CB_1 receptor, such upregulation is likely caused by an indirect effect on the ECS, since, as mentioned before, activation of the CB_1 receptor has been shown to decrease excitability and excitotoxicity on demand [119].

At present, none of the abovementioned neurobiological changes have been shown to be a biological marker, predictive for seizures outcome.

2.5 Cerebral Ischaemia

Stroke is the second most common cause of death and major cause of disability worldwide [124]. Stroke results from a transient or permanent reduction in cerebral blood flow (CBF), usually secondary to thromboembolic occlusion of one or more cerebral arteries. The compromised blood supply leads to functional impairment, followed by structural disintegration of neurons in the absence of reperfusion. The initial phase of dysfunction is potentially reversible, prior to subsequent cell death. While some brain tissue may be irreversibly damaged, other hypoperfused areas may be at risk but are potentially salvageable. These latter areas are called the penumbra [125]. If people reach their life expectancy, one in four men will have had a disabling stroke by age 80, and one in five women by age 85 [126]. The burden of stroke on patients, their families, and society in general is enormous.

The use of animal models in neuroimaging stroke research has focused on a number of areas which include: (i) defining and understanding the concept of the penumbra; (ii) development of new imaging techniques for the diagnosis and prognosis of stroke; and (iii) the investigation both of the underlying processes that lead to cell death, and of possible therapies for the treatment of stroke.

Over the last decade, comprehensive reviews have described the numerous possible animal models of cerebral ischaemia and their relevance to the human disease [127]. Experimental models may be broadly classified by the reduction in cerebral blood flow (CBF), as either global or focal models, which may in turn be permanent or reversible in nature. Models of focal ischemia most often involve unilateral, transient, or permanent occlusion of the middle cerebral artery (MCA-O), leading to ischemic damage in the neocortex and/or caudate-putamen [128]. Models of global ischemia are usually transient, since persistent global cerebral ischemia readily leads to death. Transient global ischemia can be induced with hypoxic ventilation and/or multi-vessel occlusions [129].

The penumbra is the most important target for acute stroke therapy. Since the penumbra can be considered as a temporary phase of potential viability through which ischemic tissue progresses into infarction, the therapeutic time-window is limited, possibly to a few hours; therefore early detection is essential. In humans, multitracer PET measuring blood flow and metabolism is still the current gold-standard technique for penumbral identification [130]. Diffusion/perfusion-weighted MRI and perfusion CT are more commonly used because of their simplicity and suitability for repeat studies; however, they may not differentiate infarct, penumbra and oligemia (i.e. deficiency in blood volume) reliably after stroke [130]. Following occlusion of the MCA in male spontaneously hypertensive and male normotensive Wistar Kyoto rats, CBF was decreased 1 h after the occlusion to <30 % of the control hemisphere in both groups, cerebral metabolic rate of oxygen consumption ($CMRO_2$) was diminished to a similar extent and oxygen extraction fraction (OEF) was increased, indicating misery perfusion [131]. During permanent occlusion, the underlying physiological disturbances were greater in spontaneously hypertensive rats as compared to the normotensive ones, revealing that hypertension is a risk factor for the onset of stroke as well as for poorer outcome after stroke [131]. In the same models, a collapse of the compensatory OEF mechanism was found 24 h after occlusion [132].

In rats undergoing distal MCA occlusion surgery, sequential [^{18}F]-FDG PET studies demonstrated decreased glucose metabolism in the stroke area delineated by MRI [133]. The [^{18}F]-FDG uptake in the stroke area was about 0.5 % of the injected dose per gram (ID/g) at days 1, 15 and 22. At day 8, the stroke area appeared to be smaller and the uptake was higher, likely attributable to inflammation.

Other PET studies have started to validate new ways of identifying infarction and penumbra in experimental models. [^{18}F]-FMISO PET was evaluated in rats undergoing permanent and temporary MCA occlusion [134]. Nitroimidazole compounds such as FMISO are trapped in hypoxic cells [135], but not in necrotic tissue [136], thereby providing a simple direct image of the penumbra. In the hyperacute phase (until 30 min) after permanent MCA occlusion, there was increased [^{18}F]-FMISO

binding in the entire ipsilateral MCA territory, which normalized 48 h later, in line with a nearly complete MCA territory infarct. In contrast, there was no demonstrable tracer retention in temporary MCA occlusion models, which histopathologically showed ischemic changes only, supporting the validity of [^{18}F]-FMISO as a marker of the penumbra after stroke.

Recently, Reshef et al. reported on ^{18}F-labeled-5-fluoropentyl-2-methyl-malonic acid ([^{18}F]-ML-10) as potential radioligand for imaging apoptosis among others in cerebral stroke [137]. Although necrosis predominates as the mode of cell death during the hyperacute stage of stroke, apoptosis plays an important role in ensuing staged of active disease [138]. Following permanent MCA occlusion in mice, increased [^{18}F]-ML-10 uptake was observed selectively in the ischemic MCA territory, and correlated with the histological evidence of cell death. The degree, however, to which a defective blood–brain-barrier (BBB) contribute to the specific uptake of [^{18}F]-ML-10 has not been determined.

No treatment currently exists to restore the lost neurological function after stroke. Increased vascularisation in the stroke border zone within a few days after stroke is associated with neurological recovery [139], and may be valuable not only as prognostic factor but also as measurement of success to help guide proangiogenic therapies. Using [^{64}Cu]-DOTA-VGEF$_{121}$ in rats undergoing distal MCA occlusion surgery, Cai et al. found that angiogenesis appeared very rapidly after stroke (i.e. 2 days post occlusion) [133]. [^{64}Cu]-DOTA-VGEF$_{121}$ uptake peaked in the stroke border zone ~10 days after surgery, confirmed by histology and autoradiography, after which it decreases. No correlation of [^{64}Cu]-DOTA-VGEF$_{121}$ uptake with long term stroke outcome has been performed yet to evaluate the potential prognostic value.

In a SPECT study, ^{99m}TC-HYNIC-annexin V, another radioligand for imaging apoptosis, was used to monitor the response of neuroprotective therapy with monoclonal antibody raised against FasL in a rodent model of transient MCA occlusion [140]. FasL is the cognate ligand for the Fas death receptor, a member of the tumour necrosis receptor subfamily [141]. FasL rapidly increased its expression within the neurons of the penumbra following ischemic injury, thereby inducing pro-apoptotic mechanisms [142]. Blankenberg et al. demonstrated that radiolabeled annexin V detects the early phases of neuronal ischemic injury and its response to anti-FasL therapy. Anti-FasL treatment significantly reduced annexin uptake by 92 % with a 60 % decrease in the number of apoptotic neurons on day 1. On day 6, treated rat had an 80 % reduction in tracer uptake with a 75 % decrease in infarct size as compared to controls. Annexin V uptake was in both controls and treated animals linearly correlated with infarct size and the number of apoptotic nuclei.

The same radioligand was also used in sequential SPECT studies to demonstrate the neuroprotective potential of minocycline, an antibiotic with antiapoptotic properties [143], in CB6/F1 mice undergoing unilateral distal MCA occlusion [144]. Seven-day minocycline treatment was found to significantly reduce annexin V uptake between 1 and 30 days after injury, in line with the infarct size. Annexin V uptake was in control and treated-animal maximal on days 1 and 7, followed by a decline at 30 days.

3 Applications in Psychiatry

The application of small-animal PET/SPECT in the field of biological psychiatry is hampered by the limited presence of suitable animal models. Despite a significant number of human PET/SPECT studies, there is a paucity of functional imaging studies in animals. It is indeed more difficult to reproduce human psychiatric diseases using animals in view of the large symptomatic heterogeneity of psychiatric illness, even inside the same clinical definition (endophenotypes). For example, it is particularly difficult to model specific human emotions and to evaluate this in rodents. Moreover, the aberrant behaviours symptomatic of human mental illness are mostly uniquely human, particularly those that are mediated by brain pathways without homology in rodents, e.g. the expanded prefrontal cortex of the human brain.

Despite these difficulties inherent in modelling human psychiatric phenotypes, there has been some recent success, mainly in mice, identifying genetic mutations that give rise to some of the characteristic features of anxiety, depression, schizophrenia, autism, obsessive-compulsive disorder and bipolar disorder [145]. Also here, the application of mice models in small-animal PET/SPECT research has been limited by the small size of the mouse brain. We give an overview of the various neurochemical systems that may provide possible molecular targets for small-animal PET/SPECT research.

Among the various neurotransmitter systems, the dopaminergic system is of particular interest in drug abuse and addiction. Research into brain mechanisms of additive behaviour have traditionally focused on the nucleus accumbens and dopamine inputs to this region from the ventral tegmental area [146]. The potentially significant involvements of the oribitofrontal cortex, anterior cingulate cortex, and other limbic cortical areas have more recently been recognized and investigated [147–149]. Although the precise aetiology of drug addiction is poorly understood, it is widely known to be linked to certain personality traits (e.g. risk-takers, sensation- or novelty-seekers) [150, 151] and individuals diagnosed with particular brain disorders such as attention-deficit hyperactivity disorder (ADHD) [152].

In a recent small-animal PET study, Dalley et al. investigated dopamine $D_{2/3}$ receptor availability in the dorsal and ventral striatum of high impulsive rats compared with non-impulsive rats to evaluate the causal relationship between impulsivity and drug abuse vulnerability [153]. Rats were scanned using the radioligand [^{18}F]fallypride prior to drug exposure. The authors found that [^{18}F]fallypride binding was significantly reduced in the nucleus accumbens but not the dorsal striatum of high impulsive rats compared with non-impulsive subjects. Extracellular dopamine levels were also measured in the nucleus accumbens using in vivo microdialysis [153]; there was no difference between both groups suggesting that dopamine $D_{2/3}$ receptors were likely fewer in number in the nucleus accumbens of high impulsive rats. The authors hypothesized from their PET findings that low dopamine $D_{2/3}$ receptors associated with certain personality traits may be a susceptible neurobiological marker that confers vulnerability to drug experimentation and encourage excessive drug use.

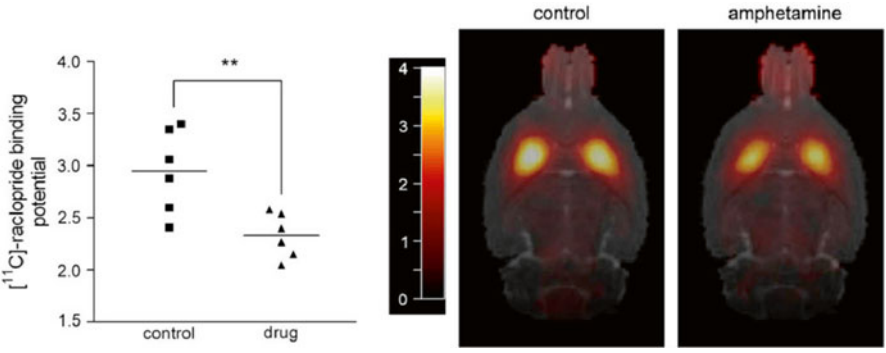

Fig. 19.3 Reduced binding potential of the dopamine $D_{2/3}$ receptor antagonist [^{11}C]-raclopride in the dorsal striatum of rats exposed to intravenous D-amphetamine self-administration compared with control rats receiving yoked infusions of saline (*left hand* graph). Shown also are co-registered [^{11}C]-raclopride binding potential maps and MRI images for a saline control rat and an amphetamine-exposed rat. **$p < 0.01$ (Student's unpaired *t*-test). Reprinted from [158], with permission from Elsevier

In addition, the origin of inter-individual variability in impulsive behaviour is still unknown, but potentially involves both genetic and environmental influences [154, 155]. The importance of environment on dopamine D_2 receptor availability was demonstrated in the monkey striatum [156]. Dopamine D_2 receptor availability measured by [^{18}F]fluoroclebopride was found to be lower in the subordinate monkeys than dominant monkeys. Crucially, this difference was present only when the monkeys were housed together—not before—suggesting this effect to be related to social context rather than to traits variables. The authors also demonstrated a link between low dopamine D_2 receptor availability in the striatum and cocaine self-administration. This finding was substantiated in a recent longitudinal PET study in the monkey brain, demonstrating that baseline dopamine D_2 receptor availability inversely predicts cocaine self-administration and that cocaine itself further reduce the dopamine D_2 receptor availability in this region [157].

This latter finding was also observed in rats, self-administering the psychostimulant D-amphetamine [158]. Drug-exposed and saline control rats were scanned 24 h after the discontinuation of self-administration using PET and [^{11}C]-raclopride. Consistent with the abovementioned study in monkey, chronic administration of amphetamine significantly decreased [^{11}C]-raclopride binding potential in the dorsal striatum (Fig. 19.3).

Besides drug abuse and addiction, molecular neuroimaging studies are also consistent with the notion that dopaminergic dysregulation is a key pathological feature of schizophrenia. Schizophrenia affects 1 % of the population [159] and usually begins in late adolescence or early adulthood. It is characterized by positive psychotic symptoms, such as delusions and hallucinations and disorganized speech, and negative psychotic symptoms, such as emotional blunting and loss of drive. PET and SPECT human imaging studies have shown that schizophrenia is associated with increased presynaptic striatal dopamine synthesis and storage [160, 161],

and increased striatal release of dopamine following amphetamine administration [162, 163]. Treatment consequently involves the use of antipsychotic drug, all of which act as antagonists at central dopamine D_2 receptors [164].

The application of small-animal PET/SPECT in schizophrenia research is mainly focused on the development and evaluation of these antipsychotic drugs for the treatment of this disorder. Despite extensive clinical experience with antipsychotics, there has long been no broad consensus on the doses of these substances that should be administered. Formerly, most antipsychotics were administered empirically according to clinical dose-finding studies, in which arbitrarily selected doses were tested to find the "most efficient" dose range in a patient population, with no regard for the molecular effects of the tested drug. Brain PET imaging studies in healthy rats have indicated that occupancy of at least 65 % of dopamine D_2 receptors is needed for clinical response to antipsychotics, and that occupancy rates exceeding 72 and 78 % are associated with a high risk for motor adverse effects, providing a rationale for the use of relatively low doses of typical antipsychotics [165].

PET studies in patients with schizophrenia that assessed the level of dopamine D_1 receptors in the prefrontal cortex using [^{11}C]SCH23390 and [^{11}C]NCC112 [166–168], have generated contradictory findings. Small-animal PET in healthy rats provided evidence to elucidate this inconsistency [169]. Sprague–Dawley rats subjected to acute dopamine depletion did not show alterations in [^{11}C]NCC112 in the striatum and prefrontal cortex, while paradoxically striatal [^{11}C]SCH23390 binding was decreased. On the other hand, subchronic dopamine depletion was associated with increased [^{11}C]NCC112 binding and decreased [^{11}C]SCH23390 binding in these regions, suggesting that the binding of these tracers in the prefrontal cortex of patients with schizophrenia might reflect changes in dopamine D_1 receptors secondary to sustained deficit in the prefrontal dopamine function.

Apart from the dopaminergic system, the central serotonergic system has received great interest in depression research [170]. Modifications of serotonergic activity contribute to many of the symptoms, for example, mood, appetite, sleep, sexual and cognitive dysfunction. Depression has the highest prevalence of all psychiatric disorders and occurs twice as frequently in women as in men. It can begin at any age, but has its average age of onset in the mid-20s [171].

The involvement of the serotonergic system in depression is also based partly on the observation that selective serotonin reuptake inhibitors (SSRIs) exert antidepressant effects and that most antidepressant drugs either directly or indirectly enhance serotonin (5-HT) transmission [172]. The most promising evidence for a deficit in central serotonin neurotransmission that is compensated by antidepressant pharmacotherapy involves postsynaptic serotonin-1A receptors (5-HT_{1A}). In human PET studies, changes in expression and function of the 5-HT_{1A} receptor are well described, particularly in the mesiotemporal cortex and raphe nucleus (for review see [173]). Currently, most of the radiopharmaceuticals developed to image 5-HT_{1A} receptors have also been validated in rodents, but not yet applied in depression research. 5-HT_{1A} receptor subtypes have been extensively visualized with small-animal PET using [^{11}C]WAY-100635 [174]. A new promising tool for the in vivo imaging of this receptor subtype in rodents is recently presented by [^{18}F]

MPPF [175]. Aznavour and colleagues demonstrated using [^{18}F]MPPF in rats that values of binding potential for hippocampus (1.2), entorhinal cortex (1.1), medial prefrontal cortex (1.0) and raphe nuclei (0.6) were comparable to those previously measured with PET in cats, non-human primates or humans [175]. Test-retest variability was also in the order of 10 % in the larger brain regions and less than 20 % in small nuclei.

Individuals affected by depression may also suffer from mania in bipolar disorder, which affects approximately 1 % of the world's population [176]. Hougland et al. performed in vivo [^{18}F]-FDG imaging in a rat model of mania [177]. Following ICV ouabain administration, brain [^{18}F]-FDG uptake was reduced compared to those animals receiving equal volumes of artificial cerebrospinal fluid. Pretreatment with lithium, a standard treatment for mania, normalized this [^{18}F]-FDG uptake. Imaging of ill bipolar patients has revealed consistent findings [178, 179].

The dopaminergic and serotonergic neurotransmitter systems have also been central in functional imaging research of patients with eating disorders. Patients with anorexia nervosa (AN) and bulimia nervosa (BN) display anxiety, depression, and suicide or have symptoms related to altered reward and excessive motor activity [180]. In human imaging studies of AN, involvement of the parietal, frontal and cingulate cortices in the pathophysiology have been well demonstrated using radioligands for the serotonergic pathways [181], as well as [^{18}F]-FDG [182].

In an animal model of AN, Barabarich-Marsteller et al. investigated using [^{18}F]-FDG whether the psychobiological changes that occur following 'voluntary' starvation in individuals are comparable to the changes that result from involuntary food restriction (i.e., an experimental procedure leading to activity-based anorexia or ABA) [183]. Briefly, rats were restricted to 40 % of their baseline daily food intake until a 30 % weight loss occurred. Combining the food restriction with access to a running wheel induced hyperactivity and a spontaneous restriction of food intake, as seen in humans [184]. Only the food-restricted rats displayed an increase in [^{18}F]-FDG uptake in the cerebellum, while a decrease was observed in the hippocampus and striatum; the latter is in line with previous reports in the clinical condition [182].

More recently, these cerebral metabolic changes in the same ABA model were monitored using a voxel-based analysis approach [185]. In line with Barabarich-Marsteller et al., a higher regional metabolism in the cerebellum and hypometabolism was found in the ventral striatum. In addition, relative [^{18}F]-FDG uptake was increased in the mediodorsal thalamus and ventral pontine nuclei, while body weight loss was positively correlated with cerebral metabolism in the cingulate cortex and the adjacent somato-sensory cortex. It was concluded that the activity-based rat model of AN share indeed several characteristics with the human disease, encompassing complex interplays between different circuitries involving motor activity, food-related behaviour and somato-sensory regions, thus adding proof to the validity of this model.

Despite the abovementioned body of evidence indicating a prominent role of dopamine and serotonin neurotransmission in various psychiatric disorders, there is a limited base of PET/SPECT studies investigating the role of other neurochemical

systems in patients or models for psychiatry. Human studies have suggested that GABAergic abnormalities are associated with stress, anxiety, and depression [186–188]. Glutamate neurotransmission, on the other hand, may be involved in obsessive compulsive behaviour and schizophrenia [189, 190]. Although radioligands to image both systems have been validated in small-animals [191, 192], none of them have yet been utilized in psychiatric animal research.

4 Conclusion

Preclinical in vivo imaging techniques such as PET and SPECT have played a role in validating animal models of neurological and psychiatric diseases at a basic science level, and therefore contributed to improve our understanding of human diseases. In particular, the key advantages of these research tools is that subjects can be followed longitudinally, over time, thus allowing investigation of the disease process, the development of compensatory changes, and the long-term evaluation of the safety and efficacy of drug-based, surgical, cellular or gene-therapy based interventions.

The preclinical evaluation of potential therapies using small-animal imaging has mainly been applied in the field of neurology. The use of small-animal PET/SPECT imaging in psychiatry is hampered by the lack of suitable animal models, as preclinical neuroimaging research is only as good as the animal model being employed.

Acknowledgments CC is a Postdoctoral Researcher for the Research Council of the Katholieke Universiteit Leuven, Belgium; KVL is Senior Clinical Researcher for the Fund for Scientific Research Flanders (FWO), Belgium. This work was funded in part by the European Community FP7-Network-of-Excellence INMiND (grant agreement no. 278850). HZ knowledge support provided by the Swiss National Science Foundation under grant SNSF 31003A-125246.

References

1. Lythgoe MF, Sibson NR, Harris NG (2003) Neuroimaging of animal models of brain disease. Br Med Bull 65:235-257.
2. Hitzemann R (2000) Animal models of psychiatric disorders and their relevance to alcoholism. Alcohol Res Health 24:149-158.
3. Burns HD, Van Laere K, Sanabria-Bohorquez S et al (2007) [18F]MK-9470, a positron emission tomography (PET) tracer for in vivo human PET brain imaging of the cannabinoid-1 receptor. Proc Natl Acad Sci U S A 104:9800-9805.
4. Chitneni SK, Garreau L, Cleynhens B et al (2008) Improved synthesis and metabolic stability analysis of the dopamine transporter ligand [(18)F]FECT. Nucl Med Biol 35:75-82.
5. Birchfield NB and Casida JE (1996) Protoporphyrinogen oxidase: high affinity tetrahydrophthalimide radioligand for the inhibitor/herbicide-binding site in mouse liver mitochondria. Chem Res Toxicol 9:1135-1139.
6. Wienhard K (2002) Measurement of glucose consumption using [(18)F]fluorodeoxyglucose. Methods 27:218-225.

7. Myers R and Hume S (2002) Small animal PET. Eur Neuropsychopharmacol 12:545-555.
8. Vastenhouw B and Beekman F (2007) Submillimeter total-body murine imaging with U-SPECT-I. J Nucl Med 48:487-493.
9. van der Have F, Vastenhouw B, Ramakers RM et al (2009) U-SPECT-II: An Ultra-High-Resolution Device for Molecular Small-Animal Imaging. J Nucl Med 50:599-605.
10. Massoud TF and Gambhir SS (2003) Molecular imaging in living subjects: seeing fundamental biological processes in a new light. Genes Dev 17:545-580.
11. Tsukada H (1999) Delivery of radioligands for positron emission tomography (PET) in the central nervous system. Adv Drug Deliv Rev 37:175-188.
12. Vaska P, Woody CL, Schlyer DJ et al (2004) RatCAP: miniaturized head-mounted PET for conscious rodent brain imaging. IEEE Trans Nucl Sci 51:2718-2722.
13. Votaw J, Byas-Smith M, Hua J et al (2003) Interaction of isoflurane with the dopamine transporter. Anesthesiology 98:404-411.
14. Matsumura A, Mizokawa S, Tanaka M et al (2003) Assessment of microPET performance in analyzing the rat brain under different types of anesthesia: comparison between quantitative data obtained with microPET and ex vivo autoradiography. Neuroimage 20:2040-2050.
15. Ingvar M, Eriksson L, Rogers GA, Stone-Elander S, Widen L (1991) Rapid feasibility studies of tracers for positron emission tomography: high-resolution PET in small animals with kinetic analysis. J Cereb Blood Flow Metab 11:926-931.
16. Laforest R, Sharp TL, Engelbach JA et al (2005) Measurement of input functions in rodents: challenges and solutions. Nucl Med Biol 32:679-685.
17. Gunn RN, Lammertsma AA, Hume SP, Cunningham VJ (1997) Parametric imaging of ligand-receptor binding in PET using a simplified reference region model. Neuroimage 6:279-287.
18. Wu HM, Huang SC, Allada V et al (1996) Derivation of input function from FDG-PET studies in small hearts. J Nucl Med 37:1717-1722.
19. Pain F, Laniece P, Mastrippolito R et al (2004) Arterial input function measurement without blood sampling using a beta-microprobe in rats. J Nucl Med 45:1577-1582.
20. Sossi V and Ruth TJ (2005) Micropet imaging: in vivo biochemistry in small animals. J Neural Transm 112:319-330.
21. Jagoda EM, Vaquero JJ, Seidel J, Green MV, Eckelman WC (2004) Experiment assessment of mass effects in the rat: implications for small animal PET imaging. Nucl Med Biol 31:771-779.
22. Casteels C, Vermaelen P, Nuyts J et al (2006) Construction and Evaluation of Multitracer Small-Animal PET Probabilistic Atlases for Voxel-Based Functional Mapping of the Rat Brain. J Nucl Med 47:1858-1866.
23. Rubins DJ, Melega WP, Lacan G et al (2003) Development and evaluation of an automated atlas-based image analysis method for microPET studies of the rat brain. Neuroimage 20:2100-2118.
24. Kesner AL, Dahlbom M, Huang SC et al (2006) Semiautomated analysis of small-animal PET data. J Nucl Med 47:1181-1186.
25. Segars WP, Tsui BM, Frey EC, Johnson GA, Berr SS (2004) Development of a 4-D digital mouse phantom for molecular imaging research. Mol Imaging Biol 6:149-159.
26. Dogdas B, Stout D, Chatziioannou AF, Leahy RM (2007) Digimouse: a 3D whole body mouse atlas from CT and cryosection data. Phys Med Biol 52:577-587.
27. Taschereau R, Chow PL, Chatziioannou AF (2006) Monte carlo simulations of dose from microCT imaging procedures in a realistic mouse phantom. Med Phys 33:216-224.
28. Stabin MG, Peterson TE, Holburn GE, Emmons MA (2006) Voxel-based mouse and rat models for internal dose calculations. J Nucl Med 47:655-659.
29. Wu L, Zhang G, Luo Q, Liu Q (2008) An image-based rat model for Monte Carlo organ dose calculations. Med Phys 35:3759-3764.
30. Zaidi H and Xu XG (2007) Computational anthropomorphic models of the human anatomy: the path to realistic Monte Carlo modeling in radiological sciences. Annu Rev Biomed Eng 9:471-500.

31. Zaidi H and Tsui BMW (2009) Review of anthropomorphic computational anatomical and physiological models. Proceedings of the IEEE 97:1938-53.
32. Beekman F, Vastenhouw B, vander Wilt G et al (2009) 3D rat phantom for ultra-high resolution molecular imaging. Proceedings of the IEEE 97:1997-2005.
33. Samii A, Nutt JG, Ransom BR (2004) Parkinson's disease. Lancet 363:1783-1793.
34. Fearnley JM and Lees AJ (1991) Ageing and Parkinson's disease: substantia nigra regional selectivity. Brain 114 (Pt 5):2283-2301.
35. Hantraye P (1998) Modeling dopamine system dysfunction in experimental animals. Nucl Med Biol 25:721-728.
36. Schapira AH (2006) Etiology of Parkinson's disease. Neurology 66:S10-S23.
37. Recchia A, Debetto P, Negro A et al (2004) Alpha-synuclein and Parkinson's disease. FASEB J 18:617-626.
38. Jenner P (2008) Functional models of Parkinson's disease: a valuable tool in the development of novel therapies. Ann Neurol 64 Suppl 2:S16-S29.
39. Doudet DJ, Chan GL, Holden JE et al (1998) 6-[18F]Fluoro-L-DOPA PET studies of the turnover of dopamine in MPTP-induced parkinsonism in monkeys. Synapse 29:225-232.
40. Yee RE, Irwin I, Milonas C et al (2001) Novel observations with FDOPA-PET imaging after early nigrostriatal damage. Mov Disord 16:838-848.
41. Melega WP, Raleigh MJ, Stout DB et al (1996) Longitudinal behavioral and 6-[18F]fluoro-L-DOPA-PET assessment in MPTP-hemiparkinsonian monkeys. Exp Neurol 141:318-329.
42. Doudet DJ, Wyatt RJ, Cannon-Spoor E et al (1993) 6-[18F]fluoro-L-dopa and cerebral blood flow in unilaterally MPTP-treated monkeys. J Neural Transplant Plast 4:27-38.
43. Eberling JL, Bankiewicz KS, Jordan S, VanBrocklin HF, Jagust WJ (1997) PET studies of functional compensation in a primate model of Parkinson's disease. Neuroreport 8: 2727-2733.
44. Eberling JL, Pivirotto P, Bringas J, Bankiewicz KS (2000) Tremor is associated with PET measures of nigrostriatal dopamine function in MPTP-lesioned monkeys. Exp Neurol 165:342-346.
45. Hume SP, Lammertsma AA, Myers R et al (1996) The potential of high-resolution positron emission tomography to monitor striatal dopaminergic function in rat models of disease. J Neurosci Methods 67:103-112.
46. Sharma SK and Ebadi M (2005) Distribution kinetics of 18F-DOPA in weaver mutant mice. Brain Res Mol Brain Res 139:23-30.
47. Sharma SK, El Refaey H, Ebadi M (2006) Complex-1 activity and 18F-DOPA uptake in genetically engineered mouse model of Parkinson's disease and the neuroprotective role of coenzyme Q10. Brain Res Bull 70:22-32.
48. Strome EM, Cepeda IL, Sossi V, Doudet DJ (2006) Evaluation of the integrity of the dopamine system in a rodent model of Parkinson's disease: small animal positron emission tomography compared to behavioral assessment and autoradiography. Mol Imaging Biol 8:292-299.
49. Sossi V, Holden JE, Topping GJ et al (2007) In vivo measurement of density and affinity of the monoamine vesicular transporter in a unilateral 6-hydroxydopamine rat model of PD. J Cereb Blood Flow Metab 27:1407-1415.
50. Nguyen TV, Brownell AL, Iris Chen YC et al (2000) Detection of the effects of dopamine receptor supersensitivity using pharmacological MRI and correlations with PET. Synapse 36:57-65.
51. Hume SP, Myers R, Bloomfield PM et al (1992) Quantitation of carbon-11-labeled raclopride in rat striatum using positron emission tomography. Synapse 12:47-54.
52. Kaasinen V, Ruottinen HM, Nagren K et al (2000) Upregulation of putaminal dopamine D2 receptors in early Parkinson's disease: a comparative PET study with [11C] raclopride and [11C]N-methylspiperone. J Nucl Med 41:65-70.
53. Nikolaus S, Larisch R, Beu M et al (2003) Bilateral increase in striatal dopamine D2 receptor density in the 6-hydroxydopamine-lesioned rat: a serial in vivo investigation with small animal PET. Eur J Nucl Med Mol Imaging 30:390-395.

54. Casteels C, Lauwers E, Bormans G, Baekelandt V, Van Laere K (2007) Metabolic-dopaminergic mapping of the 6-hydroxydopamine rat model for Parkinson's disease. Eur J Nucl Med Mol Imaging
55. Lauwers E, Beque D, Van Laere K et al (2007) Non-invasive imaging of neuropathology in a rat model of alpha-synuclein overexpression. Neurobiol Aging 28:248-257.
56. Inaji M, Okauchi T, Ando K et al (2005) Correlation between quantitative imaging and behavior in unilaterally 6-OHDA-lesioned rats. Brain Res 1064:136-145.
57. Chen YI, Brownell AL, Galpern W et al (1999) Detection of dopaminergic cell loss and neural transplantation using pharmacological MRI, PET and behavioral assessment. Neuroreport 10:2881-2886.
58. Brownell AL, Livni E, Galpern W, Isacson O (1998) In vivo PET imaging in rat of dopamine terminals reveals functional neural transplants. Ann Neurol 43:387-390.
59. Doudet DJ, Cornfeldt ML, Honey CR, Schweikert AW, Allen RC (2004) PET imaging of implanted human retinal pigment epithelial cells in the MPTP-induced primate model of Parkinson's disease. Exp Neurol 189:361-368.
60. Bjorklund LM, Sanchez-Pernaute R, Chung S et al (2002) Embryonic stem cells develop into functional dopaminergic neurons after transplantation in a Parkinson rat model. Proc Natl Acad Sci U S A 99:2344-2349.
61. Opacka-Juffry J, Ashworth S, Hume SP et al (1995) GDNF protects against 6-OHDA nigrostriatal lesion: in vivo study with microdialysis and PET. Neuroreport 7:348-352.
62. Sullivan AM, Opacka-Juffry J, Blunt SB (1998) Long-term protection of the rat nigrostriatal dopaminergic system by glial cell line-derived neurotrophic factor against 6-hydroxydopamine in vivo. Eur J Neurosci 10:57-63.
63. Olanow CW, Goetz CG, Kordower JH et al (2003) A double-blind controlled trial of bilateral fetal nigral transplantation in Parkinson's disease. Ann Neurol 54:403-414.
64. Freed CR, Greene PE, Breeze RE et al (2001) Transplantation of embryonic dopamine neurons for severe Parkinson's disease. N Engl J Med 344:710-719.
65. Minghetti L and Levi G (1998) Microglia as effector cells in brain damage and repair: focus on prostanoids and nitric oxide. Prog Neurobiol 54:99-125.
66. Ullrich O, Diestel A, Eyupoglu IY, Nitsch R (2001) Regulation of microglial expression of integrins by poly(ADP-ribose) polymerase-1. Nat Cell Biol 3:1035-1042.
67. Cicchetti F, Brownell AL, Williams K et al (2002) Neuroinflammation of the nigrostriatal pathway during progressive 6-OHDA dopamine degeneration in rats monitored by immunohistochemistry and PET imaging. Eur J Neurosci 15:991-998.
68. Sanchez-Pernaute R, Ferree A, Cooper O et al (2004) Selective COX-2 inhibition prevents progressive dopamine neuron degeneration in a rat model of Parkinson's disease. J Neuroinflammation 1:6-
69. Palombo E, Porrino LJ, Bankiewicz KS et al (1988) Administration of MPTP acutely increases glucose utilization in the substantia nigra of primates. Brain Res 453:227-234.
70. Porrino LJ, Burns RS, Crane AM et al (1987) Changes in local cerebral glucose utilization associated with Parkinson's syndrome induced by 1-methyl-4-phenyl-1,2,3, 6-tetrahydropyridine (MPTP) in the primate. Life Sci 40:1657-1664.
71. Wooten GF and Collins RC (1983) Effects of dopaminergic stimulation on functional brain metabolism in rats with unilateral substantia nigra lesions. Brain Res 263:267-275.
72. Kuhl DE, Metter EJ, Riege WH (1984) Patterns of local cerebral glucose utilization determined in Parkinson's disease by the [18F]fluorodeoxyglucose method. Ann Neurol 15:419-424.
73. Lozza C, Baron JC, Eidelberg D et al (2004) Executive processes in Parkinson's disease: FDG-PET and network analysis. Hum Brain Mapp 22:236-245.
74. Walker FO (2007) Huntington's disease. Lancet 369:218-228.
75. The Huntington's Disease Collaborative Research Group (1993) A novel gene containing a trinucleotide repeat that is expanded and unstable on Huntington's disease chromosomes. The Huntington's Disease Collaborative Research Group. Cell 72:971-983.

76. Wexler NS, Lorimer J, Porter J et al (2004) Venezuelan kindreds reveal that genetic and environmental factors modulate Huntington's disease age of onset. Proc Natl Acad Sci U S A 101:3498-3503.
77. Coyle JT and Schwarcz R (1976) Lesion of striatal neurones with kainic acid provides a model for Huntington's chorea. Nature 263:244-246.
78. Beal MF, Kowall NW, Ellison DW et al (1986) Replication of the neurochemical characteristics of Huntington's disease by quinolinic acid. Nature 321:168-171.
79. Borlongan CV, Koutouzis TK, Sanberg PR (1997) 3-Nitropropionic acid animal model and Huntington's disease. Neurosci Biobehav Rev 21:289-293.
80. Mangiarini L, Sathasivam K, Seller M et al (1996) Exon 1 of the HD gene with an expanded CAG repeat is sufficient to cause a progressive neurological phenotype in transgenic mice. Cell 87:493-506.
81. Marsh JL, Pallos J, Thompson LM (2003) Fly models of Huntington's disease. Hum Mol Genet 12 Spec No 2:R187-R193.
82. von Horsten S, Schmitt I, Nguyen HP et al (2003) Transgenic rat model of Huntington's disease. Hum Mol Genet 12:617-624.
83. Araujo DM, Cherry SR, Tatsukawa KJ, Toyokuni T, Kornblum HI (2000) Deficits in striatal dopamine D(2) receptors and energy metabolism detected by in vivo microPET imaging in a rat model of Huntington's disease. Exp Neurol 166:287-297.
84. Ishiwata K, Ogi N, Hayakawa N et al (2002) Adenosine A2A receptor imaging with [11C] KF18446 PET in the rat brain after quinolinic acid lesion: comparison with the dopamine receptor imaging. Ann Nucl Med 16:467-475.
85. Ishiwata K, Ogi N, Hayakawa N et al (2002) Positron emission tomography and ex vivo and in vitro autoradiography studies on dopamine D2-like receptor degeneration in the quinolinic acid-lesioned rat striatum: comparison of [11C]raclopride, [11C]nemonapride and [11C] N-methylspiperone. Nucl Med Biol 29:307-316.
86. Moresco RM, Lavazza T, Belloli S et al (2008) Quinolinic acid induced neurodegeneration in the striatum: a combined in vivo and in vitro analysis of receptor changes and microglia activation. Eur J Nucl Med Mol Imaging 35:704-715.
87. Brownell AL, Chen YI, Yu M et al (2004) 3-Nitropropionic acid-induced neurotoxicit--ssessed by ultra high resolution positron emission tomography with comparison to magnetic resonance spectroscopy. J Neurochem 89:1206-1214.
88. Wang X, Sarkar A, Cicchetti F et al (2005) Cerebral PET imaging and histological evidence of transglutaminase inhibitor cystamine induced neuroprotection in transgenic R6/2 mouse model of Huntington's disease. J Neurol Sci 231:57-66.
89. Fratiglioni L, De Ronchi D, Guero-Torres H (1999) Worldwide prevalence and incidence of dementia. Drugs Aging 15:365-375.
90. Jellinger KA (2008) Neuropathological aspects of Alzheimer disease, Parkinson disease and frontotemporal dementia. Neurodegener Dis 5:118-121.
91. Selkoe DJ (2002) Alzheimer's disease is a synaptic failure. Science 298:789-791.
92. Williamson J, Goldman J, Marder KS (2009) Genetic aspects of Alzheimer disease. Neurologist 15:80-86.
93. Spillantini MG, Murrell JR, Goedert M et al (1998) Mutation in the tau gene in familial multiple system tauopathy with presenile dementia. Proc Natl Acad Sci U S A 95:7737-7741.
94. Gotz J, Deters N, Doldissen A et al (2007) A decade of tau transgenic animal models and beyond. Brain Pathol 17:91-103.
95. Gotz J and Ittner LM (2008) Animal models of Alzheimer's disease and frontotemporal dementia. Nat Rev Neurosci 9:532-544.
96. Levin CS and Zaidi H (2007) Current trends in preclinical PET system design. PET Clinics 2:125-160.
97. Herholz K, Carter SF, Jones M (2007) Positron emission tomography imaging in dementia. Br J Radiol 80 Spec No 2:S160-S167.

98. Valla J, Chen K, Berndt JD et al (2002) Effects of image resolution on autoradiographic measurements of posterior cingulate activity in PDAPP mice: implications for functional brain imaging studies of transgenic mouse models of Alzheimer's Disease. Neuroimage 16:1-6.
99. Skovronsky DM, Zhang B, Kung MP et al (2000) In vivo detection of amyloid plaques in a mouse model of Alzheimer's disease. Proc Natl Acad Sci U S A 97:7609-7614.
100. Klunk WE, Engler H, Nordberg A et al (2004) Imaging brain amyloid in Alzheimer's disease with Pittsburgh Compound-B. Ann Neurol 55:306-319.
101. Bacskai BJ, Hickey GA, Skoch J et al (2003) Four-dimensional multiphoton imaging of brain entry, amyloid binding, and clearance of an amyloid-beta ligand in transgenic mice. Proc Natl Acad Sci U S A 100:12462-12467.
102. Klunk WE, Lopresti BJ, Ikonomovic MD et al (2005) Binding of the positron emission tomography tracer Pittsburgh compound-B reflects the amount of amyloid-beta in Alzheimer's disease brain but not in transgenic mouse brain. J Neurosci 25:10598-10606.
103. Maeda J, Ji B, Irie T et al (2007) Longitudinal, quantitative assessment of amyloid, neuroinflammation, and anti-amyloid treatment in a living mouse model of Alzheimer's disease enabled by positron emission tomography. J Neurosci 27:10957-10968.
104. Heneka MT, Ramanathan M, Jacobs AH et al (2006) Locus ceruleus degeneration promotes Alzheimer pathogenesis in amyloid precursor protein 23 transgenic mice. J Neurosci 26:1343-1354.
105. Fisher RS, Van Emde BW, Blume W et al (2005) Epileptic seizures and epilepsy: definitions proposed by the International League Against Epilepsy (ILAE) and the International Bureau for Epilepsy (IBE). Epilepsia 46:470-472.
106. Hauser WA and Kurland LT (1975) The epidemiology of epilepsy in Rochester, Minnesota, 1935 through 1967. Epilepsia 16:1-66.
107. Gram L (1990) Epileptic seizures and syndromes. Lancet 336:161-163.
108. The Commission on Classification and Terminology of the International League Against Epilepsy (1981) Proposal for revised clinical and electroencephalographic classification of epileptic seizures. Epilepsia 22:489-501.
109. Purpura DP, Penry JK, Woodbury DM, Tower DB, Walter RD (1972) Experimental Models of Epilepsy - A Manual for the Laboratory Worker. New York, Raven
110. Kornblum HI, Araujo DM, Annala AJ et al (2000) In vivo imaging of neuronal activation and plasticity in the rat brain by high resolution positron emission tomography (microPET). Nat Biotechnol 18:655-660.
111. Goffin K, Dedeurwaerdere S, Van Laere K, Van Paesschen W (2008) Neuronuclear assessment of patients with epilepsy. Semin Nucl Med 38:227-239.
112. Mirrione MM, Schiffer WK, Siddiq M, Dewey SL, Tsirka SE (2006) PET imaging of glucose metabolism in a mouse model of temporal lobe epilepsy. Synapse 59:119-121.
113. Wang D, Pascual JM, Yang H et al (2006) A mouse model for Glut-1 haploinsufficiency. Hum Mol Genet 15:1169-1179.
114. Dick AP, Harik SI, Klip A, Walker DM (1984) Identification and characterization of the glucose transporter of the blood-brain barrier by cytochalasin B binding and immunological reactivity. Proc Natl Acad Sci U S A 81:7233-7237.
115. Jupp B, Williams J, Binns D, Hicks R, O'Brien T (2007) Imaging small animal models of epileptogenesis. Neurology Asia 12 (supplement 1):51-54.
116. Goffin K, Van Paesschen W, Dupont P, Van Laere K (2009) Longitudinal microPET imaging of brain glucose metabolism in rat lithium-pilocarpine model of epilepsy. Exp Neurol
117. Liefaard LC, Ploeger BA, Molthoff CF et al (2009) Changes in GABAA receptor properties in amygdala kindled animals: in vivo studies using [11C]flumazenil and positron emission tomography. Epilepsia 50:88-98.
118. Di Marzo V, Melck D, Bisogno T, De Petrocellis L (1998) Endocannabinoids: endogenous cannabinoid receptor ligands with neuromodulatory action. Trends Neurosci 21:521-528.

119. Marsicano G, Goodenough S, Monory K et al (2003) CB1 cannabinoid receptors and on-demand defense against excitotoxicity. Science 302:84-88.
120. Wallace MJ, Wiley JL, Martin BR, Delorenzo RJ (2001) Assessment of the role of CB1 receptors in cannabinoid anticonvulsant effects. Eur J Pharmacol 428:51-57.
121. Wallace MJ, Martin BR, Delorenzo RJ (2002) Evidence for a physiological role of endocannabinoids in the modulation of seizure threshold and severity. Eur J Pharmacol 452:295-301.
122. Wallace MJ, Blair RE, Falenski KW, Martin BR, Delorenzo RJ (2003) The endogenous cannabinoid system regulates seizure frequency and duration in a model of temporal lobe epilepsy. J Pharmacol Exp Ther 307:129-137.
123. Goffin K, Bormans G, Casteels C et al (2008) An in vivo [(18)F]MK-9470 microPET study of type 1 cannabinoid receptor binding in Wistar rats after chronic administration of valproate and levetiracetam. Neuropharmacology
124. Murray CJ and Lopez AD (1997) Mortality by cause for eight regions of the world: Global Burden of Disease Study. Lancet 349:1269-1276.
125. Paciaroni M, Caso V, Agnelli G (2009) The Concept of Ischemic Penumbra in Acute Stroke and Therapeutic Opportunities. Eur Neurol 61:321-330.
126. Seshadri S and Wolf PA (2007) Lifetime risk of stroke and dementia: current concepts, and estimates from the Framingham Study. Lancet Neurol 6:1106-1114.
127. Wiebers DO, Adams HP, Jr., Whisnant JP (1990) Animal models of stroke: are they relevant to human disease? Stroke 21:1-3.
128. Carmichael ST (2005) Rodent models of focal stroke: size, mechanism, and purpose. NeuroRx 2:396-409.
129. McBean DE and Kelly PA (1998) Rodent models of global cerebral ischemia: a comparison of two-vessel occlusion and four-vessel occlusion. Gen Pharmacol 30:431-434.
130. Heiss WD (2000) Ischemic penumbra: evidence from functional imaging in man. J Cereb Blood Flow Metab 20:1276-1293.
131. Temma T, Kuge Y, Sano K et al (2008) PET O-15 cerebral blood flow and metabolism after acute stroke in spontaneously hypertensive rats. Brain Res 1212:18-24.
132. Temma T (2008) In-vivo positron emission tomography (PET) measurement of cerebral oxygen metabolism in small animals. Yakugaku Zasshi 128:1267-1273.
133. Cai W, Guzman R, Hsu AR et al (2009) Positron emission tomography imaging of poststroke angiogenesis. Stroke 40:270-277.
134. Takasawa M, Beech JS, Fryer TD et al (2007) Imaging of brain hypoxia in permanent and temporary middle cerebral artery occlusion in the rat using 18F-fluoromisonidazole and positron emission tomography: a pilot study. J Cereb Blood Flow Metab 27:679-689.
135. Nunn A, Linder K, Strauss HW (1995) Nitroimidazoles and imaging hypoxia. Eur J Nucl Med 22:265-280.
136. Miller GG, Ngan-Lee J, Chapman JD (1982) Intracellular localization of radioactively labeled misonidazole in EMT-6-tumor cells in vitro. Int J Radiat Oncol Biol Phys 8: 741-744.
137. Reshef A, Shirvan A, Waterhouse RN et al (2008) Molecular imaging of neurovascular cell death in experimental cerebral stroke by PET. J Nucl Med 49:1520-1528.
138. Mattson MP, Duan W, Pedersen WA, Culmsee C (2001) Neurodegenerative disorders and ischemic brain diseases. Apoptosis 6:69-81.
139. Krupinski J, Kaluza J, Kumar P, Kumar S, Wang JM (1994) Role of angiogenesis in patients with cerebral ischemic stroke. Stroke 25:1794-1798.
140. Blankenberg FG, Kalinyak J, Liu L et al (2006) 99mTc-HYNIC-annexin V SPECT imaging of acute stroke and its response to neuroprotective therapy with anti-Fas ligand antibody. Eur J Nucl Med Mol Imaging 33:566-574.
141. French LE and Tschopp J (2003) Protein-based therapeutic approaches targeting death receptors. Cell Death Differ 10:117-123.

142. Martin-Villalba A, Hahne M, Kleber S et al (2001) Therapeutic neutralization of CD95-ligand and TNF attenuates brain damage in stroke. Cell Death Differ 8:679-686.
143. Wang X, Zhu S, Drozda M et al (2003) Minocycline inhibits caspase-independent and -dependent mitochondrial cell death pathways in models of Huntington's disease. Proc Natl Acad Sci U S A 100:10483-10487.
144. Tang XN, Wang Q, Koike MA et al (2007) Monitoring the protective effects of minocycline treatment with radiolabeled annexin V in an experimental model of focal cerebral ischemia. J Nucl Med 48:1822-1828.
145. Flint J and Shifman S (2008) Animal models of psychiatric disease. Curr Opin Genet Dev 18:235-240.
146. Roberts DC, Corcoran ME, Fibiger HC (1977) On the role of ascending catecholaminergic systems in intravenous self-administration of cocaine. Pharmacol Biochem Behav 6:615-620.
147. Everitt BJ, Hutcheson DM, Ersche KD et al (2007) The orbital prefrontal cortex and drug addiction in laboratory animals and humans. Ann N Y Acad Sci 1121:576-597.
148. Hester R and Garavan H (2004) Executive dysfunction in cocaine addiction: evidence for discordant frontal, cingulate, and cerebellar activity. J Neurosci 24:11017-11022.
149. Volkow ND, Fowler JS, Wang GJ, Goldstein RZ (2002) Role of dopamine, the frontal cortex and memory circuits in drug addiction: insight from imaging studies. Neurobiol Learn Mem 78:610-624.
150. Adams JB, Heath AJ, Young SE et al (2003) Relationships between personality and preferred substance and motivations for use among adolescent substance abusers. Am J Drug Alcohol Abuse 29:691-712.
151. Dawe S and Loxton NJ (2004) The role of impulsivity in the development of substance use and eating disorders. Neurosci Biobehav Rev 28:343-351.
152. Levin FR and Kleber HD (1995) Attention-deficit hyperactivity disorder and substance abuse: relationships and implications for treatment. Harv Rev Psychiatry 2:246-258.
153. Dalley JW, Fryer TD, Brichard L et al (2007) Nucleus accumbens D2/3 receptors predict trait impulsivity and cocaine reinforcement. Science 315:1267-1270.
154. Crabbe JC and Cunningham CL (2007) Trait or state? Science 317:1033-1035.
155. Uhl G (2007) Premature poking: impulsivity, cocaine and dopamine. Nat Med 13:413-414.
156. Morgan D, Grant KA, Gage HD et al (2002) Social dominance in monkeys: dopamine D2 receptors and cocaine self-administration. Nat Neurosci 5:169-174.
157. Nader MA, Morgan D, Gage HD et al (2006) PET imaging of dopamine D2 receptors during chronic cocaine self-administration in monkeys. Nat Neurosci 9:1050-1056.
158. Dalley JW, Fryer TD, Aigbirhio FI et al (2009) Modelling human drug abuse and addiction with dedicated small animal positron emission tomography. Neuropharmacology 56 Suppl 1:9-17.
159. Lopez AD and Murray CC (1998) The global burden of disease, 1990-2020. Nat Med 4: 1241-1243.
160. Hietala J, Syvalahti E, Vilkman H et al (1999) Depressive symptoms and presynaptic dopamine function in neuroleptic-naive schizophrenia. Schizophr Res 35:41-50.
161. McGowan S, Lawrence AD, Sales T, Quested D, Grasby P (2004) Presynaptic dopaminergic dysfunction in schizophrenia: a positron emission tomographic [18F]fluorodopa study. Arch Gen Psychiatry 61:134-142.
162. Laruelle M, Bi-Dargham A, Gil R, Kegeles L, Innis R (1999) Increased dopamine transmission in schizophrenia: relationship to illness phases. Biol Psychiatry 46:56-72.
163. Breier A, Su TP, Saunders R et al (1997) Schizophrenia is associated with elevated amphetamine-induced synaptic dopamine concentrations: evidence from a novel positron emission tomography method. Proc Natl Acad Sci U S A 94:2569-2574.
164. Seeman P, Chau-Wong M, Tedesco J, Wong K (1975) Brain receptors for antipsychotic drugs and dopamine: direct binding assays. Proc Natl Acad Sci U S A 72:4376-4380.
165. Mukherjee J, Christian BT, Narayanan TK, Shi B, Mantil J (2001) Evaluation of dopamine D-2 receptor occupancy by clozapine, risperidone, and haloperidol in vivo in the rodent and nonhuman primate brain using 18F-fallypride. Neuropsychopharmacology 25:476-488.

166. Okubo Y, Suhara T, Suzuki K et al (1997) Decreased prefrontal dopamine D1 receptors in schizophrenia revealed by PET. Nature 385:634-636.
167. Karlsson P, Farde L, Halldin C, Sedvall G (2002) PET study of D(1) dopamine receptor binding in neuroleptic-naive patients with schizophrenia. Am J Psychiatry 159:761-767.
168. Bi-Dargham A, Mawlawi O, Lombardo I et al (2002) Prefrontal dopamine D1 receptors and working memory in schizophrenia. J Neurosci 22:3708-3719.
169. Guo N, Hwang DR, Lo ES et al (2003) Dopamine depletion and in vivo binding of PET D1 receptor radioligands: implications for imaging studies in schizophrenia. Neuropsychopharmacology 28:1703-1711.
170. Arango V, Underwood MD, Mann JJ (2002) Serotonin brain circuits involved in major depression and suicide. Prog Brain Res 136:443-453.
171. Doris A, Ebmeier K, Shajahan P (1999) Depressive illness. Lancet 354:1369-1375.
172. Neumeister A, Nugent AC, Waldeck T et al (2004) Neural and behavioral responses to tryptophan depletion in unmedicated patients with remitted major depressive disorder and controls. Arch Gen Psychiatry 61:765-773.
173. Drevets WC, Thase ME, Moses-Kolko EL et al (2007) Serotonin-1A receptor imaging in recurrent depression: replication and literature review. Nucl Med Biol 34:865-877.
174. Mathis CA, Simpson NR, Mahmood K, Kinahan PE, Mintun MA (1994) [11C]WAY 100635: a radioligand for imaging 5-HT1A receptors with positron emission tomography. Life Sci 55:L403-L407.
175. Aznavour N, Benkelfat C, Gravel P et al (2009) MicroPET imaging of 5-HT 1A receptors in rat brain: a test-retest [18F]MPPF study. Eur J Nucl Med Mol Imaging 36:53-62.
176. Goodwin R and Jamison KR (1990) Manic-depressive illness. Oxford University Press, New York
177. Hougland MT, Gao Y, Herman L et al (2008) Positron emission tomography with fluorodeoxyglucose-F18 in an animal model of mania. Psychiatry Res 164:166-171.
178. Baxter LR, Jr., Phelps ME, Mazziotta JC et al (1985) Cerebral metabolic rates for glucose in mood disorders. Studies with positron emission tomography and fluorodeoxyglucose F 18. Arch Gen Psychiatry 42:441-447.
179. Al-Mousawi AH, Evans N, Ebmeier KP et al (1996) Limbic dysfunction in schizophrenia and mania. A study using 18F-labelled fluorodeoxyglucose and positron emission tomography. Br J Psychiatry 169:509-516.
180. Sigel E (2008) Eating disorders. Adolesc Med State Art Rev 19:547-72, xi.
181. Bailer UF, Frank GK, Henry SE et al (2005) Altered brain serotonin 5-HT1A receptor binding after recovery from anorexia nervosa measured by positron emission tomography and [carbonyl11C]WAY-100635. Arch Gen Psychiatry 62:1032-1041.
182. Delvenne V, Lotstra F, Goldman S et al (1995) Brain hypometabolism of glucose in anorexia nervosa: a PET scan study. Biol Psychiatry 37:161-169.
183. Barbarich-Marsteller NC, Marsteller DA, Alexoff DL, Fowler JS, Dewey SL (2005) MicroPET imaging in an animal model of anorexia nervosa. Synapse 57:85-90.
184. Casper RC, Sullivan EL, Tecott L (2008) Relevance of animal models to human eating disorders and obesity. Psychopharmacology (Berl) 199:313-329.
185. Van Kuyck K, Casteels C, Vermaelen P et al (2007) Motor- and food-related metabolic cerebral changes in the activity-based rat model for anorexia nervosa: A voxel-based microPET study. Neuroimage 35:214-221.
186. Tokunaga M, Ida I, Higuchi T, Mikuni M (1997) Alterations of benzodiazepine receptor binding potential in anxiety and somatoform disorders measured by 123I-iomazenil SPECT. Radiat Med 15:163-169.
187. Kaschka W, Feistel H, Ebert D (1995) Reduced benzodiazepine receptor binding in panic disorders measured by iomazenil SPECT. J Psychiatr Res 29:427-434.
188. Geuze E, van Berckel BN, Lammertsma AA et al (2008) Reduced GABAA benzodiazepine receptor binding in veterans with post-traumatic stress disorder. Mol Psychiatry 13:74-83, 3.
189. McGuire P, Howes OD, Stone J, Fusar-Poli P (2008) Functional neuroimaging in schizophrenia: diagnosis and drug discovery. Trends Pharmacol Sci 29:91-98.

190. Rosenberg DR, Mirza Y, Russell A et al (2004) Reduced anterior cingulate glutamatergic concentrations in childhood OCD and major depression versus healthy controls. J Am Acad Child Adolesc Psychiatry 43:1146-1153.
191. Dedeurwaerdere S, Gregoire MC, Vivash L et al (2009) In-vivo imaging characteristics of two fluorinated flumazenil radiotracers in the rat. Eur J Nucl Med Mol Imaging
192. Shetty HU, Zoghbi SS, Simeon FG et al (2008) Radiodefluorination of 3-fluoro-5-(2-(2-[18F](fluoromethyl)-thiazol-4-yl)ethynyl)benzonitrile ([18F]SP203), a radioligand for imaging brain metabotropic glutamate subtype-5 receptors with positron emission tomography, occurs by glutathionylation in rat brain. J Pharmacol Exp Ther 327:727-735.